

Article

Experimental Study on Mineral Dissolution and Carbonation Efficiency Applied to pH-Swing Mineral Carbonation for Improved CO₂ Sequestration

Natalia R. Galina ^{1,*} , Gretta L. A. F. Arce ¹, Mercedes Maroto-Valer ² and Ivonete Ávila ¹ 

¹ Laboratory of Combustion and Carbon Capture (LC3), Department of Energy and Chemistry, School of Engineering, UNESP—São Paulo State University, Av. Dr. Ariberto Pereira da Cunha, 333, Guaratinguetá 12516-410, SP, Brazil

² Research Centre for Carbon Solutions (RCCS), School of Engineering & Physical Sciences, Heriot-Watt University, Edinburgh EH14 4AS, UK

* Correspondence: natalia-ribeiro.galina@unesp.br

Abstract: Mineral carbonation incurs high operating costs, as large amounts of chemicals and energy must be used in the process. Its implementation on an industrial scale requires reducing expenditures on chemicals and energy consumption. Thus, this work aimed to investigate the significant factors involved in pH-swing mineral carbonation and their effects on CO₂ capture efficiency. A central composite rotatable design (CCRD) was employed for optimizing the operational parameters of the acid dissolution of serpentinite. The results showed that temperature exerts a significant effect on magnesium dissolution. By adjusting the reaction temperature to 100 °C and setting the hydrochloric acid concentration to 2.5 molar, 96% magnesium extraction was achieved within 120 min of the reaction and 91% within 30 min of the reaction. The optimal efficiency of carbon dioxide capture was 40–50%, at higher values than those found in literature, and 90% at 150 bar and high pressures. It was found that it is technically possible to reduce the reaction time to 30 min and maintain magnesium extraction levels above 90% through the present carbonation experiments.

Keywords: mineral carbonation; pH swing; serpentinite; CCUS; central composite rotatable design



Citation: Galina, N.R.; Arce, G.L.A.F.; Maroto-Valer, M.; Ávila, I. Experimental Study on Mineral Dissolution and Carbonation Efficiency Applied to pH-Swing Mineral Carbonation for Improved CO₂ Sequestration. *Energies* **2023**, *16*, 2449. <https://doi.org/10.3390/en16052449>

Academic Editors: Federica Raganati and Paola Ammendola

Received: 13 November 2022

Revised: 13 January 2023

Accepted: 9 February 2023

Published: 4 March 2023



Copyright: © 2023 by the authors. Licensee MDPI, Basel, Switzerland. This article is an open access article distributed under the terms and conditions of the Creative Commons Attribution (CC BY) license (<https://creativecommons.org/licenses/by/4.0/>).

1. Introduction

Anthropogenic activities, especially energy production and transport, significantly contribute to increases in greenhouse gas (GHG) emissions. To avert climate change and the concomitant temperature rise, anthropogenic CO₂ emissions must be reduced to less than 20 GtCO₂ a year by 2050 [1]. In addition to reducing CO₂ emissions, net-negative processes to remove large amounts of CO₂ from the atmosphere are worth mentioning [1,2]. Alkaline materials rich in silicate and hydroxide minerals from industrial activities will have stored from 2.9 to 8.5 billion tons of CO₂ yearly by 2100 in the form of solid carbonate minerals [2].

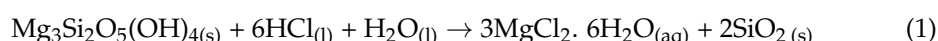
The carbon capture process can be implemented by three types of operational methods: pre-combustion, post-combustion, and oxy-fuel combustion. The process of mineral carbonation refers to post-combustion capture. In such a case, CO₂ is captured in exhaust gases as fuel is fully burned with air [3]. In a recent study, a comparative techno-economic analysis was carried out for these three types of operation methods. It was found that post-combustion stands out from a financial standpoint, since it causes less disruption to existing operational methods and therefore a lower expenditure due not having to shut down and revamp plants [4]. It should be noted, however, that the study in question did not address mineral carbonation.

Mineral carbonation is a promising technology in the context of reducing CO₂ emissions into the atmosphere [5–7], due to an abundance of raw materials and its long-term

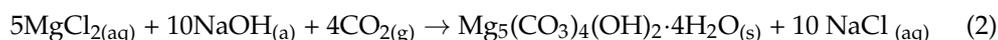
CO₂ storage capacity [6,8,9]. It involves carbon capture, utilization, and storage (CCUS), as it is a technological approach for controlling anthropogenic CO₂ emissions into the atmosphere. By injecting CO₂ into host rocks, geological formations react, and large amounts of CO₂ are stored as carbonate minerals. [10].

pH-swing indirect mineral carbonation takes place in three main stages: (1) dissolution/extraction, (2) purification, and (3) CO₂ capture by carbonation. Mineral dissolution is more efficient in acidic environments, while mineral carbonation presents better results in basic pH conditions ranging between 9 and 11 [11,12].

In the first stage of the process (dissolution), the solution pH is reduced to acidic levels and reactive components (Mg, Fe, and Ca) are extracted from the raw material (rocks or industrial waste). According to the literature [13–16], solutions of hydrochloric acid (HCl) show high efficiency in serpentinite dissolution. The serpentinite dissolution reaction using HCl solution occurs according to Equation (1) [17].



After the dissolution stage, the solution pH is adjusted to basic levels using basic solutions and CO₂ is injected after the solution pH is stabilized to form carbonates [18]. According to Arce et al. [19], there is high efficiency in using HCl in the stage of dissolution and NaOH as the base in the carbonation stage, but high energy costs are incurred to recover these reagents. Hemmati et al. [12] used an HCl/NaOH system to study the process of mineral carbonation in aqueous media. Their results achieved carbonation efficiency of 82.5%. The carbonation reaction using NaOH to adjust the solution pH to basic levels occurs according to Equation [2], with the reaction product being hydromagnesite (Mg₅(CO₃)₄(OH)₂·4H₂O) [20].



The main products obtained from the mineral carbonation process are magnetite (Fe₃O₄), in the purification stage of the solution obtained from serpentine rock dissolution, in addition to various carbonates such as magnesite, MgCO₃, nesqueonite, MgCO₃·2H₂O, and hydromagnesite (Mg₅(CO₃)₄(OH)₂·4H₂O), in the stage of CO₂ capture [12]. These products can be obtained using different process configurations.

There are other approaches in the literature to mineral carbonation processes in addition to the pH-swing method, with each one offering advantages and disadvantages. Table 1 presents a brief comparison of such approaches.

Table 1. Comparison of different types of mineral carbonation processes.

Types of Carbonation	Advantage	Disadvantage	Application
pH-Swing	Shorter reaction time; greater efficiency	Two or more reactors; regeneration of chemical additives; large water consumption in regeneration stages	It cannot be currently applied due to its large energy consumption in additive regeneration stages
Aqueous Mineral Carbonation	A single reactor	Additive regeneration; non-reusable chemical additives; impure carbonates	Difficult applicability due to the level of complexity to regenerate used additives
Gas–Solid Mineral Carbonation	A single reactor; simple process	Very slow kinetics	Non-applicable due to very slow reaction rates

Mineral carbonation is a sophisticated technology that includes in-situ and ex-situ processes [11], in which the first processes involve the transportation and injection of CO₂ into rocks and the second processes occur through a carbonation reaction in industrial reactors after the mechanical activation of the raw material that reacts with CO₂ [7]. A literature

review revealed that ex-situ aqueous mineral carbonation is a viable option to reach small and average emissions in places where geological storage is unfeasible [7–9,12–14].

In indirect ex-situ mineral carbonation, the metals of interest are initially extracted from the raw material through an acid dissolution reaction, but a reaction with CO₂ to form carbonate precipitates might then occur [9,12,15]. Serpentine dissolution reactions and carbonate production occur at different pH conditions [9,16–19]. A swing in pH (pH-swing process) from acidic to basic conditions in metal extraction during carbonate precipitation is essential to increase conversion rates and obtain high-purity products [20].

Different acid/base systems were investigated [17–19,21,22]. Although the HCl/NaOH system is efficient during the dissolution and carbonation steps, the large energy consumption necessary to recover both HCl and NaOH is a major disadvantage [17]. The regeneration of reagents is the most energy-consuming step and directly contributes to raising operating costs [23], as the water evaporation that occurs during regeneration requires a large amount of heat, which in turn leads to an increased energy penalty [24,25]. The heat demand for water evaporation in the HCl/NaOH system is 1908 MJ/t CO₂ storage [26]. Thus, in order for the mineral carbonation process to be economically viable, water consumption must be reduced in the process [24].

According to certain authors [12,17,27], large amounts of chemical additives are used in indirect mineral carbonation, thus requiring recovery. The pH-swing method arose as an alternative method for the recovery and reuse of additives in the process, increasing the silicate dissolution efficiency and reducing the costs incurred in the mineral carbonation process. However, the energy consumption associated with the recovery steps of chemical additives is high, both in HCl/NaOH and NH₄HSO₄/NH₄OH systems [12,18]. As a result, research has been carried out with the aim of minimizing the energy consumption.

Rashid et al. [27] indicate that the significant energy consumption in these processes is due to the fact that large amounts of water must be evaporated before recovering additives. In the context of HCl/NaOH systems, Bu et al. [28] stated that bipolar electro dialysis processes can be performed at ambient temperatures, thus producing aqueous solutions of 1 M HCl and NaOH and requiring 372–569 kWh/tNaOH, which can reduce energy penalties when compared to conventional electro dialysis processes [29].

Stokreef et al. [30] indicated that a NH₄HSO₄/NH₄OH system requires 1300 kWh/tCO₂ to evaporate water and regenerate ammonium salts. A study conducted by Sanna et al. [31] revealed that the use of liquid–liquid extraction to regenerate chemical additives might reduce energy consumption by 35% (845 kWh/tCO₂) when compared to conventional evaporation processes.

The HCl/NaOH process appears to be the most promising with regard to energy efficiency. Although HCl/NaOH systems require no water evaporation, the use of large amounts of water could incur environmental costs.

A large consumption of energy, the use of chemicals, and low efficiency involved in fixing CO₂ in the form of carbonates are factors affecting the total cost of the process [5–7,31]. According to Hitch and Dipple [32], there must be a balance between the efficiency of CO₂ sequestration and the amount of CO₂ emitted as a result of the process, so as to make mineral carbonation economically viable.

The commercial application of mineral carbonation processes is limited due to slow reaction rates and low energy efficiency; however, the capacity to reduce CO₂ emissions on a global scale must still be researched in the context of mineral carbonation [33].

According to Zhang et al. [33], aqueous mineral carbonation requires smoother process parameters than gas–solid mineral carbonation, in addition to offering more opportunities for intensification through chemical additives, catalysts, and process integration.

However, the large consumption of water is a significant environmental liability that must be overcome in aqueous mineral carbonation. Veetil and Hitch [7] reported a consumption of 3.2 tons of water for each ton of wollastonite used in indirect aqueous mineral carbonation. Water is an indispensable resource in the production process. Therefore, in

order to make production processes cleaner and eco-industrial parks viable, technologies minimizing water consumption are of paramount importance [34].

In light of this, this work aimed to investigate how the control variables of mineral carbonation processes can affect acid dissolution efficiency and, consequentially, carbonation steps in a Brazilian serpentinite sample. Unprecedented data were acquired through the use of this Brazilian serpentinite in ex-situ mineral carbonation. The use of NaOH in solid phase was explored in order to reduce water consumption and improve MgCO_3 formation efficiency. This approach has been poorly explored in the literature on mineral carbonation. For the acid dissolution step, a central composite rotatable design (CCRD) was used to determine and control the main factors affecting Mg extraction. After determining the optimal operating conditions for the acid dissolution process, the influence of the acid dissolution reaction time was investigated in order to reduce its energy consumption. In the step of CO_2 mineralization, the behavior of the CO_2 capture reaction under atmospheric and high pressures was investigated.

2. Materials and Methods

2.1. Raw Material

The raw material used in this research was serpentinite (SERP). It was provided by SAMA Mining and found in the Cana Brava mine located in the city of Minaçu in the state of Goiás, Brazil. The material was processed through two consecutive standard ASTM 60 and 70 sieves (250–212 μm), and particles ranging between 212 and 250 μm in size were obtained.

Figure 1 shows the XRD (X-ray diffraction) pattern for the SERP sample. Its results indicate that SERP is heterogeneous and composed of three minerals, namely (a) lizardite ($\text{Mg}_3\text{Si}_2(\text{OH})_4\text{O}_5$), (b) hematite (Fe_2O_3), and (c) clinochrysotile ($\text{Mg}_3\text{Si}_2\text{O}_5(\text{OH})_4$). According to the Rietveld refinement presented by Vieira et al. [11] of the same raw material that was used in this work, SERP consists of 99.97% serpentine, 75.83% chrysotile, and 0.03% hematite.

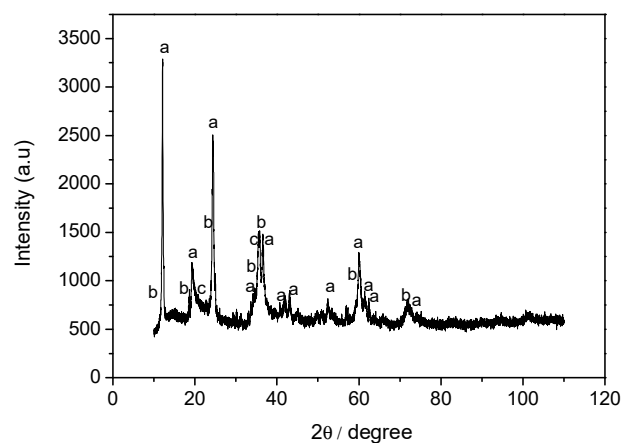


Figure 1. XRD diffractograms of mineral phase peaks detected in SERP. Where a: lizardite 1T, b: hematite and c: clinochrysotile.

An X-ray fluorescence analysis (XRF) was performed in order to determine the elemental composition. Table 2 shows the concentrations (%) of oxides present in the SERP sample obtained by XRF. The concentrations of elements present in the SERP samples obtained by inductively-coupled plasma optical emission spectrometry (ICP-OES) are also presented in Table 2. Iron (Fe), magnesium (Mg), calcium (Ca), and silicon (Si) are the main elements making up the raw material. Other metals such as aluminum (Al), chrome (Cr), and nickel (Ni) are present in the sample, but they are considered impurities. These impurities, as well as Fe, must be removed from the solution before the carbonation process occurs so as to enhance the formation of pure Mg carbonates [19].

Table 2. Chemical composition of SERP.

Oxides	XRF Concentration (%)	Elements	ICP-OES * Concentration (%)
MgO	37.09	Mg	23
Al ₂ O ₃	1.62	Al	0.35
SiO ₂	44.23	Si	8.4
CaO	2.79	Ca	279.5
Cr ₂ O ₃	0.84	Cr	n.d
Fe ₂ O ₃	12.82	Fe	4.49
NiO	0.58	Ni	n.d

* Source: adapted from Arce et al. [17].

2.2. pH Swing Process

A simplified flowchart of the three main steps of CO₂ sequestration by pH-swing mineral carbonation is illustrated in Figure 2, including (1) the dissolution favored in acidic environments; (2) purification for the purpose of the precipitation of impurities at pH conditions ranging between 5 and 9, and (3) the carbonation occurring in basic environments [35]. In this research, HCl was used since it leads to a high serpentinite dissolution efficiency [18,20,22,36].

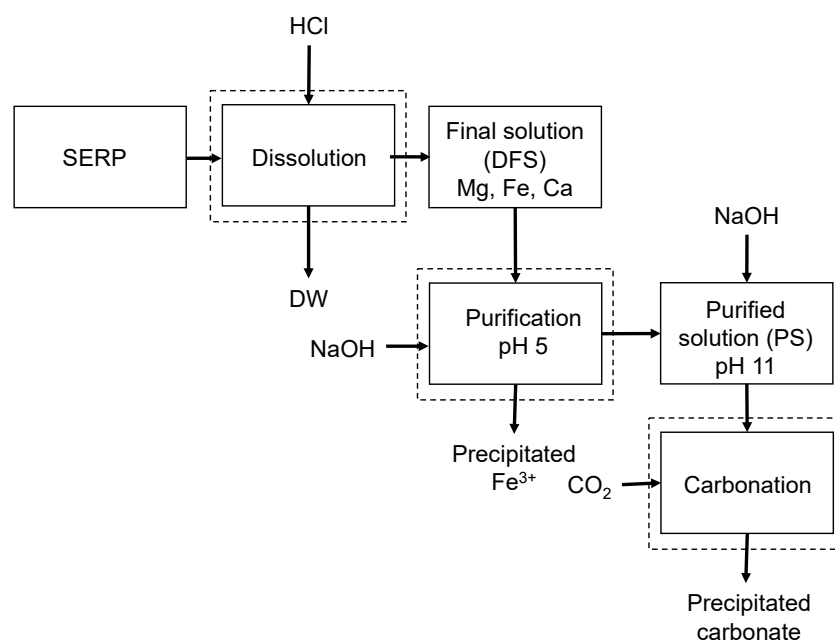


Figure 2. Simplified flowchart of CO₂ sequestration by pH-swing mineral carbonation.

The experimental bench for obtaining carbonates was set up considering the three stages of the process, and the carbonation stage was carried out under atmospheric conditions at high pressures.

As for the acid dissolution step, a 250 mL borosilicate glass reactor equipped with a 300 mm-long serpentine-type glass condenser was used in order to avoid losses due to HCl evaporation. To stir and heat the solution within the reactor, a magnetic stirrer with heating and digital temperature control was used with an encapsulated thermometer and a 250 mm-long magnetic stirrer.

With respect to the purification stage, a 250 mL Erlenmeyer flask and a magnetic stirrer were used in order to maintain constant agitation. A 50 mL burette was used to add the base (NaOH) by dripping. The solution pH was adjusted with a pH and temperature transmitter.

Concerning the carbonation stage, tests were carried out at atmospheric pressure (1 atm), and a reaction system was set up consisting of a 250 mL borosilicate glass reactor, a heating magnetic stirrer, a digital temperature control with an encapsulated thermometer, a 250 mm long magnetic stirrer, and a 300 mm-long serpentine-type glass condenser. The solution pH was adjusted by means of a pH and temperature transmitter. Mineral carbonation tests under high pressure conditions were carried out at the Research Center for Carbon Solutions (RCCS) of Heriot-Watt University. A high-pressure, high-temperature (HTHP) reactor coated with polytetrafluoroethylene (PTFE) was used. The solution pH was adjusted before closing the system, and temperature control was performed using a heating jacket.

2.2.1. Dissolution of Minerals

Acid dissolution experiments were carried out under stoichiometric conditions and atmospheric pressure. A total of 100 mL of hydrochloric acid (HCl) was introduced into the glass reactor and heated whilst stirring. The heating temperature and concentration of HCl (C_{HCl}) in each experiment were determined according to an experimental design. The SERP sample was inserted into a glass reactor when the system reached the temperature determined through an experimental design, with it being kept under heating and rotation. Afterwards, the solution was filtered using a vacuum system in order to separate the residue (DW) from the final solution (DFS). The Mg concentration was determined using atomic absorption (AA) and ICP-OES tests, and the extraction efficiency was determined according to Equation (3).

$$\text{EXi}\% = \left[\frac{C_{\text{is}}}{C_{\text{iserp}}} \right] \cdot 100 \quad (3)$$

In Equation (3), EXi% is the fraction of Mg extracted in the acid dissolution process, C_{is} is Mg concentration in the DFS, and C_{iserp} refers to Mg concentration in the SERP.

2.2.2. Purification

In order to generate high-purity products in the carbonation step, it is necessary to purify DFS so as to remove impurities such as Fe. The pH was adjusted in two stages. Firstly, NaOH was added to the DFS under agitation to raise the pH to 5 in order to precipitate impurities as Fe^{3+} [19]. In the second stage, the solution pH was raised to 9 in order to precipitate Fe^{2+} in the form of $\text{Fe}(\text{OH})_2$ [17,19].

After the solution purification step, NaOH was used to raise the pH of the PS solution from 9 to 11 so as to prepare it for the carbonation step. It was reported in the literature that Mg precipitation begins to occur from pH 9 [19] and the highest rate of Mg conversion into carbonates is observed at pH 10 [37], whilst the highest efficiency in Mg conversion into carbonates occurs at pH conditions ranging between 8 and 11. The authors also observed that CO_2 raises the solution pH to acidic levels; thus, the pH must be adjusted to 12 in order to convert Mg into carbonates [18].

2.2.3. Mineral Carbonation

Table 3 shows the experimental conditions investigated in the mineral carbonation step. The CB1, CB2, and CB3 experiments were carried out under atmospheric pressure conditions, and the CB4, CB5, and CB5 experiments occurred under high-pressure conditions in order to control and keep the reaction parameters constant. The following equipment was used: a heating magnetic stirrer, a digital temperature control with an encapsulated thermometer, Mettler Toledo M200 pH Analytical Transmitter (produced in Brazil) and a Brooks Instrument 4800 Series Mass Flow Controller (produced in the USA). After assembling the experimental bench, PS was introduced into a glass reactor and heated until it reached the desirable temperature. Afterwards, CO_2 was injected into the solution at a volumetric flow rate of 21 mL/min within 10 min. After CO_2 injection, a pH reduction

from 11 to 8 was observed and NaOH was used to raise the solution pH to pH 11, and the reaction time was maintained at 30 min.

Table 3. Experimental conditions of the mineral carbonation process.

Experiments	Temperature	Pressure	C _{NaOH}	pH
CB1	70	1 atm	50%	11
CB2	90	1 atm	50%	11
CB3	90	1 atm	solid (2.5 g)	11
CB4	70	100 bar	solid (0.8 g)	11
CB5	90	100 bar	solid (0.8 g)	11
CB6	90	150 bar	solid (0.8 g)	11

Before setting the experimental conditions presented in Table 3, a previous exploratory study had been carried out by varying the temperature, NaOH concentration, and the volume of injected CO₂ with the aim of adjusting the methodology and ensuring repeatability in terms of carbonate precipitation. It was observed that carbonate precipitation was affected by the analyzed parameters. The results showed a tendency towards the formation of Mg(OH)₂, although hydromagnesite was obtained using 50% NaOH solution to regulate its pH conditions, but only 27 g of a low-purity product was obtained. A tendency to form Mg(OH)₂ might be related to the degree of NaOH dissociation, as it is a strong base that completely dissociates into Na⁺ and OH⁻ ions in an aqueous solution [38]. Considering this characteristics of the base being used, the possibility of using solid NaOH was investigated, and the results showed that the obtained product was pure hydromagnesite.

A high-pressure, high-temperature (HTHP) reactor coated with polytetrafluoroethylene (PTFE) was used for the high-pressure carbonation experiments. The PS was introduced into the reactor and heated to the specified temperature. After the temperature process was reached, CO₂ was injected to reach desirable pressure and then maintained for 30 min.

After the carbonation reaction was complete, the solution was filtered using a vacuum system. The precipitate obtained was then washed with deionized water and dried in an oven at 105 °C for 12 h. The carbonation step efficiency was determined according to Equation (4), which expresses the conversion of magnesium ions into carbonates determined by the mass ratio of f magnesium carbonate formed (m_{Mg}^{cb}) to magnesium present in the used solution (m_{Mg}^{DS}). The mass of CO₂ fixed in the carbonate was determined by thermogravimetric analysis (TGA), as previously reported [17].

$$X\%_{cb} = \left[\frac{m_{Mg}^{cb}}{m_{Mg}^{DS}} \right] \cdot 100 \quad (4)$$

2.3. Experimental Design: Dissolution Stage

The response surface methodology is a statistical tool used to model and analyze problems where different variables affect the response. It is used to identify the variables affecting the response and optimize the process [39]. Thus, experiments were carried out to define the effects of T (°C) and C_{HCl} on Mg extraction.

The response surface methodology coupled with second-order central composite rotatable design (CCRD) was used in order to evaluate factors affecting Mg dissolution. CCRD is a factorial design in experiments used to investigate the effects of multiple variables through conducting fewer experiments [40].

In the present study, the factors considered in the experimental design were x₁ (temperature, T°C) and x₂ (HCl concentration, C_{HCl}), evaluated at 5 levels ($\sqrt{-2}$; -1; 0; +1; $+\sqrt{2}$) in accordance with the CCRD [41] considering an experimental range discussed in previous research [19,22,29]. Table 4 shows the factors and levels studied in the acid dissolution process. A total of 13 acid dissolution experiments were carried out under the conditions determined previously, with five repetitions at the central point (0;0).

Table 4. Factors and levels of the experimental design.

Factors	Description	Level				
		$-\sqrt{2}$	-1	0	$+1$	$+\sqrt{2}$
x_1	Temperature, T (°C)	30	40	65	90	100
x_2	HCl concentration, C_{HCl} (M)	1	1.44	2.5	3.5	4

A quadratic model was obtained from the responses of experiments. Equation (5) presents the second-order response surface model [42].

$$\hat{y} = b_0 + b_1x_1 + b_2x_2 + b_{11}x_1^2 + b_{22}x_2^2 + b_{12}x_1x_2 \quad (5)$$

In the above equation, x_1 and x_2 are the independent variables related to factors by the regression model coefficients. The effect of factors (temperature and concentration of HCl) on Mg extraction was carried out through an analysis of variance based on experimental results.

3. Results and Discussion

3.1. Dissolution Step

Table 5 shows the experimental conditions used in 13 experiments conducted to determine the Mg concentration in acid dissolution solution.

Table 5. Experimental conditions and Mg concentration.

Experiments	Coded Factors		Numeric Factors		Response
	x_1	x_2	T (°C)	C_{HCl} (M)	% Mg
1	-1	-1	40	1.4	61
2	$+1$	-1	90	1.4	79
3	-1	$+1$	40	3.5	34
4	$+1$	$+1$	90	3.5	91
5	$-\sqrt{2}$	0	30	2.5	29
6	0	$+\sqrt{2}$	65	4	84
7	$+\sqrt{2}$	0	100	2.5	96
8	0	$-\sqrt{2}$	65	1	82
9	0	0	65	2.5	85
10	0	0	65	2.5	85
11	0	0	65	2.5	85
12	0	0	65	2.5	85
13	0	0	65	2.5	85

In this research, Mg is the element of interest for the carbonation step, with this therefore being the most desirable experimental condition for the acid dissolution process obtained in experiment 7, in which 96% of Mg extraction was achieved after 2 h of reaction. Teir et al. [22] achieved 93% Mg extraction in the acid dissolution process of serpentinite using 2 M HCl within 2 h of the reaction. Hemmati et al. [19] used 1 M HCl for dissolving mineral-rich forsterite and lizardite and obtained 93% Mg extraction after 6 h of reaction.

The effects of input variables on the response were analyzed statistically at a significance level of 95%. The analysis of variance (ANOVA) and a regression test (R^2) were performed to verify the model adequacy. Table 6 shows the regression model and ANOVA results for Mg extraction.

Table 6. ANOVA and regression results for Mg extraction.

Variable	Sum of Squares	df	Mean Square	F	p-Value	R ²
x ₁	3549.94	1	3549.94	135.85	0	n.d
x ₂	22	1	22	0.84	0.389	n.d
x ₁₂	1118.2	1	1118.2	42.79	0	n.d
x ₂₂	44.65	1	44.65	1.71	0.232	n.d
x ₁ x ₂	386.32	1	386.32	14.78	0.006	n.d
Model	5081.94	5	1016.39	38.89	0	96.53%
Residue	182.92	7	26.13	n.d	n.d	
Total	5264.86	12	438.73	n.d	n.d	

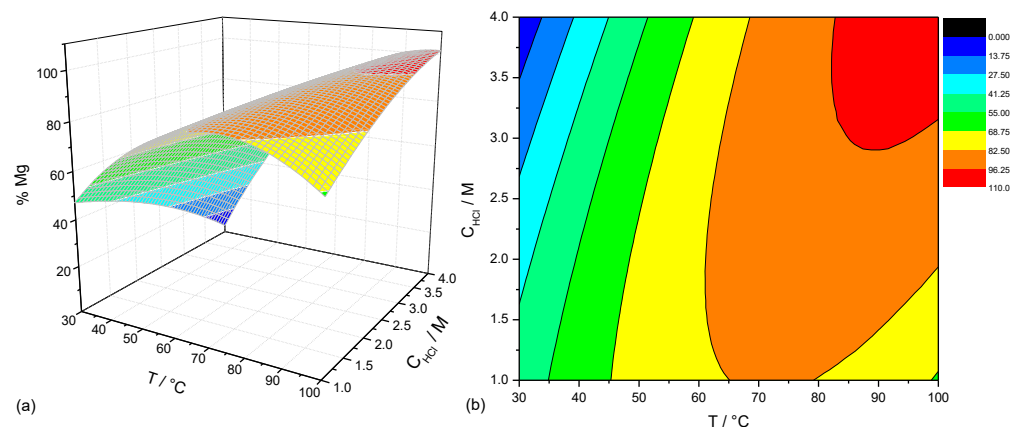
n.d, not detected.

The ANOVA reveals that the model is significant, as the value of F (38.89) is higher than that found for F tabulated according to the Fisher–Snedecor 5% F-distribution table in addition to the fact that *p*-value was less than 5%. The results of input variables *x*₁ and *x*₂ indicate that temperature has a significant influence on the response, i.e., Mg extraction in the acid dissolution process occurs as a function of temperature. The effect of temperature can be observed in the central point experiments (65 °C; 2.5 M) and experiment 7 (100 °C; 2.5 M). For the same C_{HCl}, an average of 85% Mg extraction was reached at 65 °C. By raising the process temperature to 100 °C, Mg extraction increased to 96%, which reveals that the model can explain the 96% variation in terms of Mg extraction in the acid dissolution process, i.e., the model is well adjusted to the process.

The empirical function describing the relationship between factors and Mg extraction is presented in Equation (6). It can be used to determine the optimal point of the process or predict the response variable (*y*) values considering other temperature and HCl concentration conditions unexplored experimentally.

$$y (\text{Mg}) = 85.17 + 21.07x_1 - 1.66x_2 - 12.68 x_1^2 - 2.53x_2^2 + 9.83x_1x_2 \quad (6)$$

The Mg extraction response surface was obtained from the regression equation. Figure 3 shows the response surface and contour curves of the surface of Mg extraction. The analysis suggests that the region of maximum Mg extraction is above the maximum limits of temperature (100 °C) and HCl concentration (4 M) used herein. Thus, the region of maximum Mg extraction and temperatures above 100 °C can only be reached under high pressure and temperature conditions (HPHT).

**Figure 3.** (a) Response surface and (b) contour lines of the Mg extraction process.

3.2. Effect of Time on Acid Dissolution

The acid dissolution process efficiency was evaluated as a function of time. These tests were carried out in triplicate. The experimental conditions were those in which the highest Mg extraction was obtained, i.e., 100 °C and 2.5 M HCl. The evaluated acid dissolution

reaction times were 5, 15, 30, 60, 90, 120, and 180 min, and Mg extraction was evaluated as a function of time (t) as showed in Figure 4.

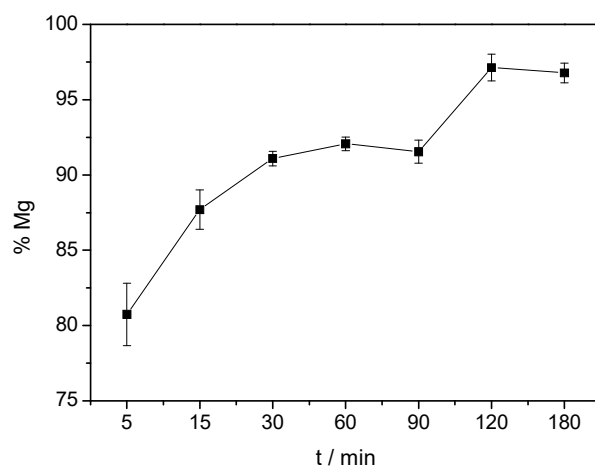


Figure 4. Mg extraction process curve as a function of reaction time.

The results show that approximately 82% Mg is extracted from serpentinite after 5 min. Between 30 to 90 min, Mg extraction remains at approximately 91%, and the Mg extraction at approximately 96% between 120 and 180 min. It is observed that there is a tendency for Mg extraction to stabilize at approximately 91% after 30 min of reaction. However, an increase of approximately 5% was observed after 120 min, which was unexpected since carbonation is a slow process whose advance speed decreases as time passes, with it thus tending towards stabilization. Other factors concerning reaction conditions might have produced variations in the process and increased extraction rates; however, a 5% increase from 30 min of reaction is considered insignificant if compared to that found during 120 min of reaction. These results indicate that for the evaluated sample and process conditions, the acid dissolution step can reach 80% extraction within 5 min of reaction.

According to Sanna et al. [43], serpentinite dissolution is the limiting, as well as being the most costly, step of the carbonation process. Thus, it is considered that a reduction in the acid dissolution time from 120 to 30 min can lower the average cost of the mineral carbonation process, while at the same time maintaining Mg extraction levels above 90%. Nonetheless, sensitivity and economic analyses should be carried out in future studies to confirm these results.

It is worth mentioning that the physico-chemical characteristics of the material under study affect Mg extraction. Arce et al. [44] evaluated the acid dissolution process of a Brazilian serpentinite which had a high lizardite content. Even though a material with a particle size of 300 μm under stoichiometric conditions was used, the results showed that high concentrations of Mg (88%) could be extracted using HCl within 30 min of reaction.

XRD diffractograms for SERP and residues (DW) obtained from different dissolution experiments are shown in Figure 5. It can be observed that structural changes in the material increase as a function of mineral extraction. In the case of the shortest experiment (5 min) with the lowest Mg extraction, the mineral phases remain crystalline, in addition to the fact that there is a reduction in the intensity of lizardite and clinochrysotile phases. After 15 min of reaction, the material is amorphized, which becomes more intense as acid dissolution increases. For the longest experiments (120 and 180 min), an extraction of Mg of approximately 96% was reached, with it still being possible to observe the presence of lizardite and clinochrysotile phases.

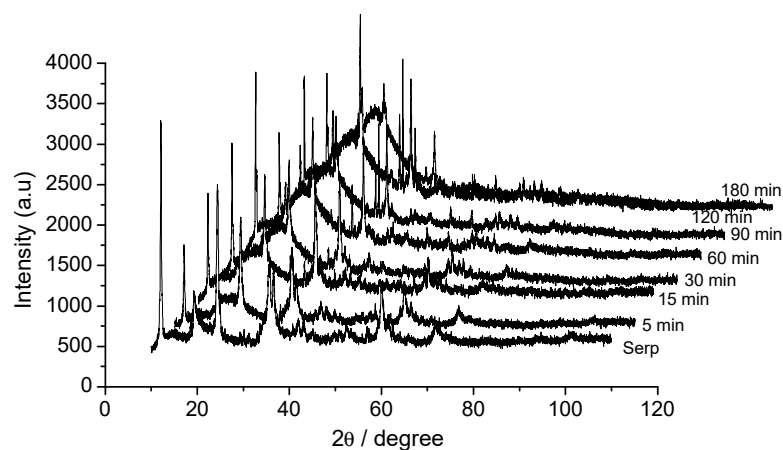


Figure 5. XRD diffractograms of SERP and DW as a function of reaction time.

The XRF analysis revealed that residues are mainly composed of SiO_2 (Figure 6), as previously observed by Hemmati et al. [19].

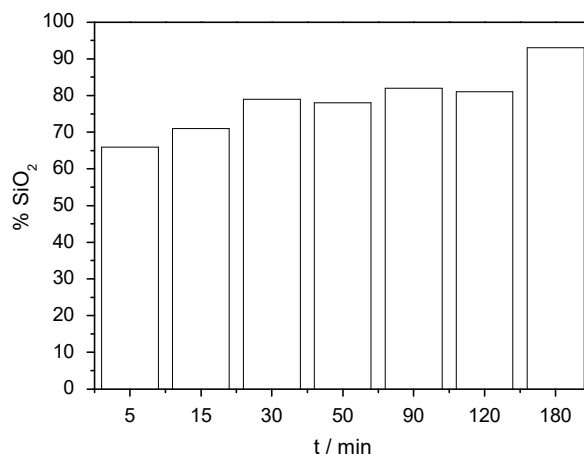


Figure 6. SiO_2 concentration in DW as a function of dissolution time.

Figure 6 shows that SiO_2 formation increases proportionally to Mg extraction and material structure transformation. Moreover, there is a tendency for it to stabilize after 30 min of reaction, and another unexpected increase occurs at 180 min. There was an approximate 10% SiO_2 extraction increase after 30 min of reaction, given that an increase in SiO_2 in the residue is expected for longer extraction times. A longer reaction time leads to a greater efficiency in terms of extracting alkaline earth metals from the host rock, i.e., Mg, which will in turn increase the SiO_2 concentration in the residue. The literature shows that it took up to 6 h of reaction time in order for SiO_2 (96–99%) purification to occur in the residue [45]. An increased concentration of silicon in the DW residue only demonstrates that there was greater efficiency in extracting Mg from the structure.

3.3. Mineral Carbonation Step

Given that a solution with 88% Mg was obtained (DFS30) after 30 min of acid dissolution reaction, this was used for the mineral carbonation step. The pH of DFS30 was raised to 5 using 15 mL of NaOH 50% for precipitating impurities such as iron. The DFS30 was filtered to remove the precipitate, and its pH condition was raised once more to 9 using 2 mL of NaOH 50%. Upon reaching a pH of 9, Fe^{2+} precipitation in the form of $\text{Fe}(\text{OH})_2$ was expected, as reported by other authors [17,19]. However, raising the solution pH led to no Fe^{2+} precipitation. Figure 7 shows the precipitates obtained at (a) pH 5 and (b) pH 9.

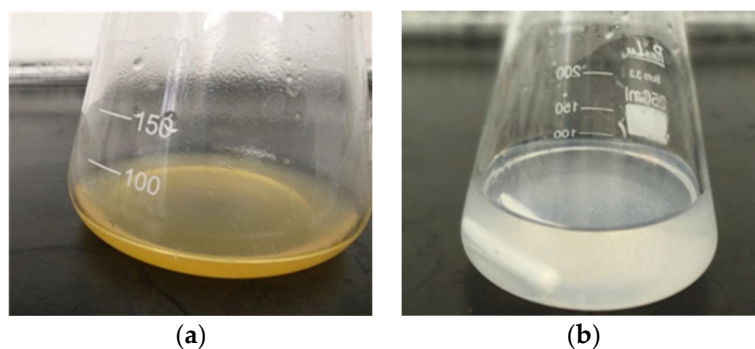


Figure 7. Precipitates obtained from the purification process at (a) pH 5 and (b) pH 9.

The purified solution (PS30) was then used in the mineral carbonation step so as to investigate the effect of pressure. The precipitates formed in the mineral carbonation step were characterized by FTIR, XRD, and TGA.

Figures 8 and 9 show the XRD patterns and FTIR spectra, respectively, of carbonation products from CB1, CB2, and CB3.

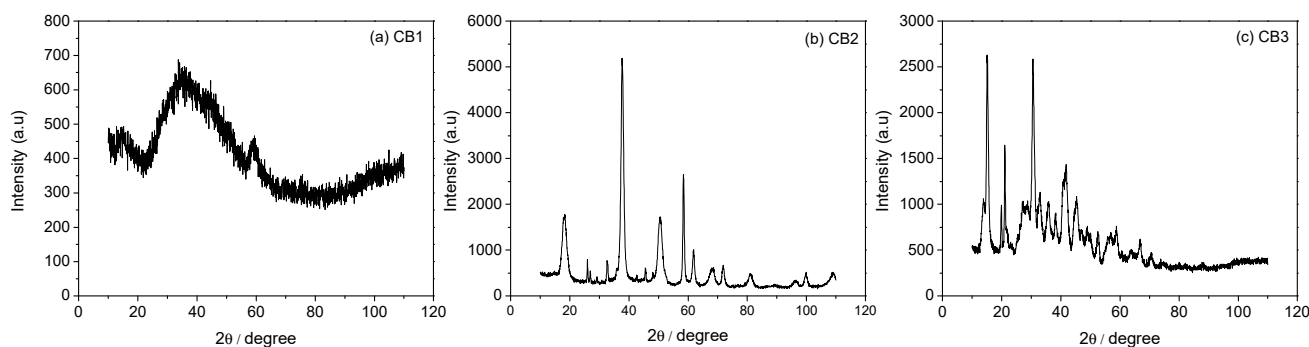


Figure 8. XRD patterns of (a) CB1, (b) CB2, and (c) CB3 products under atmospheric pressure.

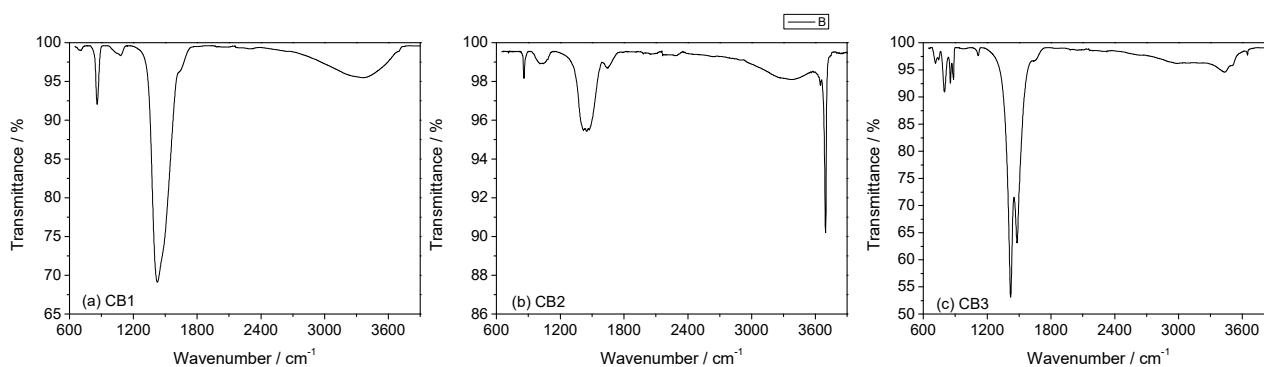


Figure 9. FTIR spectra of (a) CB1, (b) CB2, and (c) CB3 products under atmospheric pressure.

Under atmospheric pressure, the formation of three different products was observed, which are: (CB1) an unidentified amorphous precipitate; (CB2) $\text{Mg}(\text{OH})_2$, and (CB3) hydro-magnesite. For the CB1 and CB2 experiments, 50% NaOH solution was used to raise the PS solution pH to 11. The XRD analysis results indicate the formation of an amorphous product (amorphous carbonate) which was not identified in experiment CB1. For CB2, the process temperature was raised to 90 °C, and the XRD and FTIR analyses results reveal the formation of magnesium hydroxide, $\text{Mg}(\text{OH})_2$ [46]. The tendency to form $\text{Mg}(\text{OH})_2$ might be due to a dissociation of NaOH base into Na^+ and OH^- ions in an aqueous solution. Solid particles of NaOH were used to control the pH in order to reduce the degree of dissociation

in experiment CB3, whose results showed that the obtained product was hydromagnesite ($\text{Mg}_5(\text{CO}_3)_4(\text{OH})_2 \cdot 4\text{H}_2\text{O}$).

The FTIR spectra for the CB3 experiments are similar to those for hydromagnesite presented by Sanna and Maroto-Valer [36], thus confirming that CO_2 was captured as hydromagnesite, $\text{Mg}_5(\text{CO}_3)_4(\text{OH})_2 \cdot 4\text{H}_2\text{O}$ (Equation (2)). Absorption bands at approximately 600 to 900 cm^{-1} correspond to carbonate (CO_3) vibration mode outside the plane. The band at approximately 1100 cm^{-1} corresponds to the symmetric stretching vibration of CO, while those at approximately 1433 cm^{-1} and 1485 cm^{-1} correspond to asymmetric CO vibration [36].

The effect of pressure on CO_2 carbonation was evaluated for the CB4, CB5, and CB6 experiments using the same temperature range as that used for the atmospheric pressure CB1, CB2, and CB3 experiments. Figures 10 and 11 show XRD patterns and FTIR spectra, respectively, of products obtained from CB4, CB5, and CB6. An analysis of the XRD pattern indicates the formation of magnesite ($\text{MgO} + \text{CO}_2 \leftrightarrow \text{MgCO}_3$) in the CB4 experiment. The FTIR absorption spectrum shows vibrations corresponding to MgCO_3 , thus confirming that CO_2 was captured as magnesite [47]. For both the CB5 and CB6 experiments, the process temperature was raised to $90 \text{ }^\circ\text{C}$, while the pressures were maintained at 100 and 150 bar for CB5 and CB6 experiments, respectively. The XRD and FTIR analyses indicate that CO_2 was converted into hydromagnesite in both experiments.

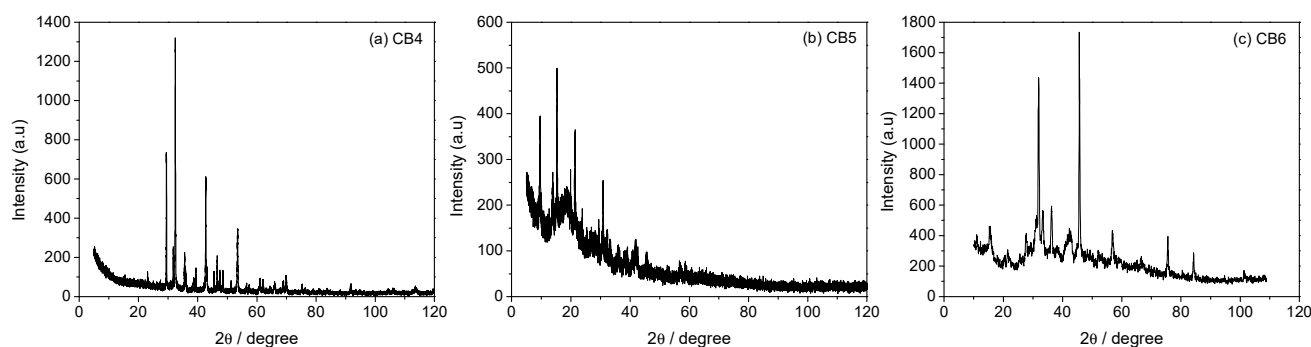


Figure 10. XRD patterns of (a) CB4, (b) CB5, and (c) CB6 products under atmospheric pressure.

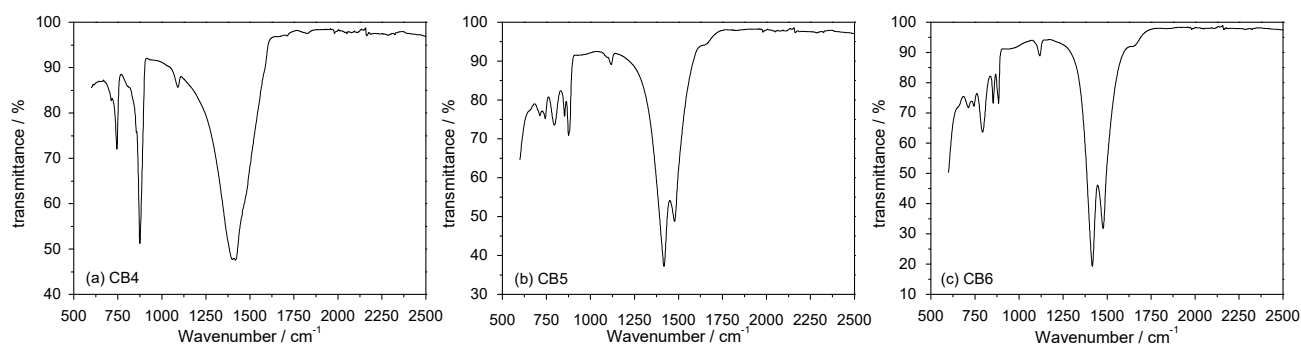


Figure 11. FTIR spectra of (a) CB4, (b) CB5, and (c) CB6 products under atmospheric pressure.

Figure 12 shows TGA and DTG curves of the thermal decomposition of products formed in the CB3, CB4, CB5, and CB6 experiments. Hydromagnesite decomposes endothermically in three mass loss events: The loss of water crystallization, hydroxide ion decomposition, and the release of CO_2 by carbonate decomposition [48–50].

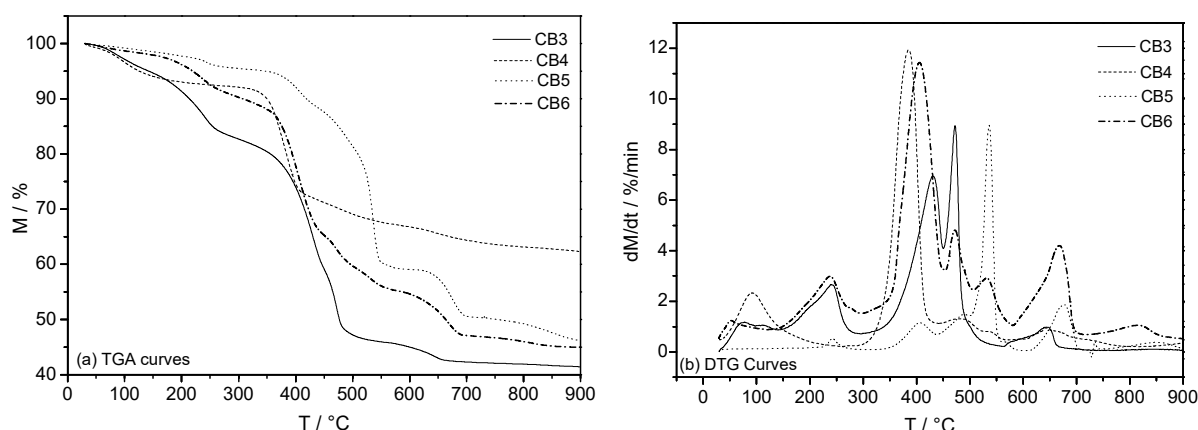


Figure 12. (a) TGA and (b) DTG curves of products obtained from the CB3, CB4, CB5, and CB6 experiments.

Magnesium carbonate still recrystallizes exothermically at high heating rates [48]. Carbonates are decomposed in two steps, and the latter occurs at higher temperatures. The decomposition event of the remaining magnesium carbonate occurs at temperatures of over 520 °C, and its occurrence depends on the reaction atmosphere and heating rate [49].

Figure 11 shows that thermal decomposition begins at approximately 300 °C. Carbonate decomposition is divided into two events, and the maximum decomposition rate of the first carbonate decomposition event occurs at 470 °C, with this occurring between 560–660 °C with respect to the second event.

The total mass loss of formed carbonates was 58%, 43%, 55%, and 55% for CB3, CB4, CB5, and CB6, respectively. The mass of CO₂ fixed in the form of carbonate corresponds to an average of 40% in the CB3, CB4, CB5, and CB6 experiments.

Table 7 lists the carbonation efficiencies (Equation (2)). In experiments CB1 and CB2, the CO₂ reaction formed no carbonates, and its efficiency was not determined. In the CB1 experiment, an amorphous product, i.e., a carbonate unidentified (u.d.) in XRD analyses, was obtained. In the CB2 experiment, magnesium hydroxide, Mg(OH)₂, was obtained, and the results show that the conversion of Mg ions into carbonate was favored under high pressure (CB4, CB5, and CB6), with the process efficiency being greater than under atmospheric pressure. An increase in CO₂ pressure generally raises the solubility of materials and facilitates carbonic acid dissociation. Thus, the concentration of carbonate ions in the solution is increased, which favors the formation of carbonates [50].

Table 7. Products of the mineral carbonation process.

Experiments	Product	Efficiency
CB1	Amorphous u.d.	n.d
CB2	Mg(OH) ₂	n.d
CB3	Hydromagnesite	66%
CB4	Magnesite (MgCO ₃)	78%
CB5	Hydromagnesite	76%
CB6	Hydromagnesite	90%

Note: n.d.: non-detected; u.d.: unidentified.

It can be seen that in high-pressure experiments, the temperature affects the type of product formed, but the process efficiency remains unaltered. For the experiment at 100 bar, magnesium carbonate and hydromagnesite were obtained at 70 °C and 90 °C, respectively. For these experiments (CB4 and CB5), the process efficiency reached similar values, i.e., 78% and 76% for CB4 and CB5, respectively. Raising the process pressure from 100 to 150 bar and maintaining process temperature at 90 °C resulted in an efficiency increase of 90%.

Although these results demonstrate that the process can produce magnesium carbonates, adjustments to process factors are still necessary to raise its efficiency. The average

the process efficiency values are below those attained by other processes reported in the literature [16–18]; however, factors such as the type of acid and base used in serpentine acid dissolution and carbonation steps, respectively, can affect process efficiency [18]. As shown by Herring et al. [50], products obtained by the carbonation reaction progress and are related to the microstructural features of the material. Thus, the mineralogical characteristics of the sample used can also explain such results.

Another factor influencing the carbonation yield is the reaction pH conditions. Purified solution was introduced into the reactor at a pH of 11. However, after the carbonation process, the pH of the remaining solution was 7.4. The maximum conversion of magnesium ions to carbonates (97%) was reached when the carbonation reaction occurred at a pH of 10; thus, the carbonation reaction pH is the main factor affecting the purity and yield in terms of carbonation [19].

Considering the optimal efficiency results of magnesium ions conversion into carbonates, 3.2 ton of serpentine will sequester 1 ton of CO₂ under the experimental conditions for CB6. The water consumption to sequester 1 ton of CO₂ is approximately 132 m³ when 50% NaOH solution is used in the steps of purification and carbonation. When considering the use of NaOH in solid phase instead of a 50% NaOH solution to regulate the pH in the purification and carbonation steps, the general water consumption is reduced to approximately 82 m³.

Table 8 shows a comparison of the state-of-the-art research papers on carbon dioxide capture efficiency.

Table 8. Comparison of state-of-the-art literature on carbon dioxide capture efficiency.

Process Type	System	t (min)	T (°C)	p (Bar)	X _{cb} (%)	Reference
pH swing	MgCl ₂ -CO ₂ -NaOH-H ₂ O	30	90	100	76%	This study
				150	90%	
pH swing	MgCl ₂ -CO ₂ -NH ₃ -H ₂ O	60	70	10	43.5%	[51]
				20	60.9%	
				30	66.7%	
				60	68.6%	
pH Swing *	MgSO ₄ -NaOH-CO ₂ -H ₂ O	10	20	40	55%	[52]
Aqueous carbonation *	EDTA	420	120	20	80%	[53]

* data collected from Rashid et al. [27].

According to Rashid et al. [27], the mineral carbonation processes at elevated pressures were mainly conducted through a single-step aqueous carbonation. However, studies addressing mineral carbonation under high pressure by the pH-swing method have not been explored in the literature. In Table 8, a comparison of the results achieved by other authors is made, although these studies achieved efficiencies of 80% within 7 h of reaction time under high pressures [53]. This appears to vary while applying pressures in pH-swing processes, as can be observed in Table 8. The carbonation time drastically reduced, but so did the carbonation efficiency, which is possibly due to the fact that all these studies were performed at pressures lower than 60 bar [51,54].

According to Zhang et al. [54], in a MgCl₂-CO₂-NH₃-H₂O system, pressures of over 30 bar slightly affect the carbonation efficiency, and the main carbonate obtained is nesquehonite. Hemati et al. [19,45] indicated that among all the carbonates that are produced, magnesite and hydromagnesite are those with the greatest potential for CO₂ capture and that their formation greatly depends on the carbonation temperature. Thus, in order to verify the carbonation efficiency, this study was carried out at temperatures ranging between 70 °C and 90 °C under high pressures.

Considering the challenges to be faced, the mineral carbonation process has high operating costs due to the consumption of large amounts of energy, water, and chemical

products [7,31]. Another challenge posed with regard to the cost-effective implementation of this process relates to increasing the reaction speed so that CO₂ can be fixed at the same rate as it is generated while burning fossil fuels. [31,53]. According to Azdarpour et al. [9], the consumption of chemicals in the carbonation process increases its total cost, and this is one of the main challenges to be faced in order to reduce the consumption of chemicals. Thus, aligning the reduction and reaction time with an increased acid concentration is a solution that penalizes the process and increases energy and acid recovery costs.

An evaluation of the acid dissolution process as a function of time showed that it is possible to reduce the dissolution reaction time from 120 min to 30 min while maintaining Mg extraction levels above 90% for the used serpentinite. It should be noted that a reduction in reaction time may contribute to reducing the process energy costs, which possibly enables the use of this technology on an industrial scale at a competitive cost.

The high energy and environmental costs of mineral carbonation processes remains a predicament, with it not yet being possible to realistically apply such processes, given that there is still a lack of economic studies in the literature.

4. Conclusions

This work investigated the steps of acid dissolution and carbonate precipitation through aqueous mineral carbonation using the pH-swing method with the aim of determining adjustments in the process that can increase the CO₂ capture efficiency while at the same time reducing the impacts of energy and water consumption. Acid dissolution is an important step in mineral carbonation; thus, this research investigated the factors affecting mineral extraction the response through the CCRD.

The experimental design allowed for the identification of the effects of both variables assessed, i.e., temperature (°C) and HCl concentration (M), on Mg extraction. The ANOVA results showed that the response surface methodologies are significant and adequately explain the process of Mg extraction. It was also found that temperature (°C) has a significant influence on Mg extraction. Mg extraction was 85% and 96% at the same HCl concentration (2.5 M) by raising the process temperature from 65 °C to 100 °C, respectively.

The highest Mg extraction (96%) was obtained at 100 °C and a HCl concentration of 2.5 M. The maximum Mg extraction was determined by the CCRD, which allowed for the discovery of how the acid dissolution reaction of serpentinite behaves as a function of time. The results showed that 82% of Mg extraction was achieved after 5 min of reaction. Extraction levels above 90% were observed after 30 min of reaction. It was also observed that within 120 min and 180 min of the reaction, the extraction remained constant, at approximately 96%. These results indicate that it is possible to reduce the time taken to dissolve serpentinite from 120 min to 30 min whilst maintaining Mg extraction levels above 90%.

Regarding mineral carbonation, the feasibility of using the solution obtained within 30 min of acid dissolution reaction was investigated. The carbonation step was investigated under atmospheric and high-pressure conditions using the NaOH base as a means to regulate the pH. The use of solid NaOH instead of a 50% NaOH solution was proposed, and the results generally indicate that the process is capable of capturing CO₂ in the form of carbonates under the investigated conditions. However, adjustments to regulate the pH must be made to investigate whether it is possible to increase the process efficiency as a result. An in-depth assessment of the process life cycle, an economic analysis, and an analysis of the technical gains resulting from reducing the acid dissolution reaction time should be studied in future works.

Author Contributions: Conceptualization, N.R.G., G.L.A.F.A., M.M.-V. and I.Á.; methodology, N.R.G.; formal analysis, M.M.-V. and I.Á.; investigation, N.R.G.; data curation, G.L.A.F.A.; writing—original draft preparation, N.R.G.; writing—review and editing, N.R.G.; supervision, M.M.-V. and I.Á. All authors provided critical feedback and helped shape the research, analysis, and manuscript. All authors have read and agreed to the published version of the manuscript.

Funding: This research was funded by the Coordenação de Aperfeiçoamento de Pessoal de Nível Superior—Brasil (CAPES)—grant number 1681464 and 88881.361902/2019-01. The authors are also grateful to FAPESP for project number 2016 /15749-5 and PRH-ANP project number 48610.20073/2019-21 PRH-ANP 34.1.

Acknowledgments: The authors would like to thank Mineração Associada (SAMA S.A.) for supplying the materials.

Conflicts of Interest: The authors declare no conflict of interest.

References

1. Mac Dowell, N.; Fennell, P.S.; Shah, N.; Maitland, G.C. The Role of CO₂ Capture and Utilization in Mitigating Climate Change. *Nat. Clim. Chang.* **2017**, *7*, 243–249. [[CrossRef](#)]
2. Renforth, P. The Negative Emission Potential of Alkaline Materials. *Nat. Commun.* **2019**, *10*, 1401. [[CrossRef](#)] [[PubMed](#)]
3. Kanniche, M.; Gros-Bonnivard, R.; Jaud, P.; Valle-Marcos, J.; Amann, J.M.; Bouallou, C. Pre-Combustion, Post-Combustion and Oxy-Combustion in Thermal Power Plant for CO₂ Capture. *Appl. Therm. Eng.* **2010**, *30*, 53–62. [[CrossRef](#)]
4. Kheirininik, M.; Ahmed, S.; Rahmanian, N. Comparative Techno-Economic Analysis of Carbon Capture Processes: Pre-Combustion, Post-Combustion, and Oxy-Fuel Combustion Operations. *Sustainability* **2021**, *13*, 13567. [[CrossRef](#)]
5. Galina, N.R.; Arce, G.L.A.F.; Ávila, I. Evolution of Carbon Capture and Storage by Mineral Carbonation: Data Analysis and Relevance of the Theme. *Miner. Eng.* **2019**, *142*, 105879. [[CrossRef](#)]
6. Neeraj; Yadav, S. Carbon Storage by Mineral Carbonation and Industrial Applications of CO₂. *Mater. Sci. Energy Technol.* **2020**, *3*, 494–500. [[CrossRef](#)]
7. Veetil, S.P.; Hitch, M. Recent Developments and Challenges of Aqueous Mineral Carbonation: A Review. *Int. J. Environ. Sci. Technol.* **2020**, *17*, 4359–4380. [[CrossRef](#)]
8. Olajire, A.A. A Review of Mineral Carbonation Technology in Sequestration of CO₂. *J. Pet. Sci. Eng.* **2013**, *109*, 364–392. [[CrossRef](#)]
9. Azdarpour, A.; Asadullah, M.; Mohammadian, E.; Hamidi, H.; Junin, R.; Karaei, M.A. A Review on Carbon Dioxide Mineral Carbonation through PH-Swing Process. *Chem. Eng. J.* **2015**, *279*, 615–630. [[CrossRef](#)]
10. Hills, C.D.; Tripathi, N.; Carey, P.J. Mineralization Technology for Carbon Capture, Utilization, and Storage. *Front. Energy Res.* **2020**, *8*, 1–14. [[CrossRef](#)]
11. Vieira, K.R.M.; Arce, G.L.A.F.; Luna, C.M.R.; Facio, V.O.; Carvalho, J.A.; Neto, T.G.S.; Ávila, I. Understanding the Acid Dissolution of Serpentinites (Tailings and Waste Rock) for Use in Indirect Mineral Carbonation. *South African J. Chem. Eng.* **2022**, *40*, 154–164. [[CrossRef](#)]
12. Sanna, A.; Uibu, M.; Caramanna, G.; Kuusik, R.; Maroto-Valer, M.M. A Review of Mineral Carbonation Technologies to Sequester CO₂. *Chem. Soc. Rev.* **2014**, *43*, 8049–8080. [[CrossRef](#)] [[PubMed](#)]
13. Bobicki, E.R.; Liu, Q.; Xu, Z.; Zeng, H. Carbon Capture and Storage Using Alkaline Industrial Wastes. *Prog. Energy Combust. Sci.* **2012**, *38*, 302–320. [[CrossRef](#)]
14. Kemache, N.; Pasquier, L.; Cecchi, E.; Mouedhen, I.; Blais, J.; Mercier, G. Aqueous Mineral Carbonation for CO₂ Sequestration: From Laboratory to Pilot Scale. *Fuel Process. Technol.* **2017**, *166*, 209–216. [[CrossRef](#)]
15. Benhelal, E.; Imran, M.; Rayson, M.S.; Prigge, J.; Molloy, S.; Brent, F.; Cote, A.; Stockenhuber, M.; Kennedy, E.M. Study on Mineral Carbonation of Heat Activated Lizardite at Pilot and Laboratory Scale. *J. CO₂ Util.* **2018**, *26*, 230–238. [[CrossRef](#)]
16. Sanna, A.; Dri, M.; Maroto-Valer, M. Carbon Dioxide Capture and Storage by PH Swing Aqueous Mineralisation Using a Mixture of Ammonium Salts and Antigorite Source. *Fuel* **2013**, *114*, 153–161. [[CrossRef](#)]
17. Arce Ferrufino, G.L.A.; Okamoto, S.; Dos Santos, J.C.; de Carvalho, J.A.; Avila, I.; Romero Luna, C.M.; Gomes Soares Neto, T. CO₂ Sequestration by PH-Swing Mineral Carbonation Based on HCl/NH₄OH System Using Iron-Rich Lizardite 1T. *J. CO₂ Util.* **2018**, *24*, 164–173. [[CrossRef](#)]
18. Teir, S.; Kuusik, R.; Fogelholm, C.-J.; Zevenhoven, R. Production of Magnesium Carbonates from Serpentine for Long-Term Storage of CO₂. *Int. J. Miner. Process.* **2007**, *85*, 1–15. [[CrossRef](#)]
19. Hemmati, A.; Shayegan, J.; Bu, J.; Yeo, T.Y.; Sharratt, P. Process Optimization for Mineral Carbonation in Aqueous Phase. *Int. J. Miner. Process.* **2014**, *130*, 20–27. [[CrossRef](#)]
20. Park, A.-H.H.A.; Fan, L.-S.S. CO₂ Mineral Sequestration: Physically Activated Dissolution of Serpentine and PH Swing Process. *Chem. Eng. Sci.* **2004**, *59*, 5241–5247. [[CrossRef](#)]
21. Wang, X.; Maroto-valer, M.M. Dissolution of Serpentine Using Recyclable Ammonium Salts for CO₂ Mineral Carbonation. *Fuel* **2011**, *90*, 1229–1237. [[CrossRef](#)]
22. Teir, S.; Revitzer, H.; Eloneva, S.; Fogelholm, C.-J.J.; Zevenhoven, R. Dissolution of Natural Serpentine in Mineral and Organic Acids. *Int. J. Miner. Process.* **2007**, *83*, 36–46. [[CrossRef](#)]
23. Yuen, Y.T.; Sharratt, P.N.; Jie, B. Carbon Dioxide Mineralization Process Design and Evaluation: Concepts, Case Studies, and Considerations. *Environ. Sci. Pollut. Res.* **2016**, *23*, 22309–22330. [[CrossRef](#)] [[PubMed](#)]
24. Wang, X.; Maroto-Valer, M.M. Optimization of Carbon Dioxide Capture and Storage with Mineralisation Using Recyclable Ammonium Salts. *Energy* **2013**, *51*, 431–438. [[CrossRef](#)]

25. Dri, M.; Sanna, A.; Maroto-Valer, M.M. Mass and Energy Balance of NH₄-Salts PH Swing Mineral Carbonation Process Using Steel Slag. *Energy Procedia* **2014**, *63*, 6544–6547. [[CrossRef](#)]
26. Teir, S. *Fixation of Carbon Dioxide by Producing Carbonates from Minerals and Steelmaking Slags*; Helsinki University of Technology: Espoo, Finland, 2008.
27. Rashid, M.I.; Benhelal, E.; Farhang, F.; Oliver, T.K.; Stockenhuber, M.; Kennedy, E.M. Application of a Concurrent Grinding Technique for Two-Stage Aqueous Mineral Carbonation. *J. CO₂ Util.* **2020**, *42*, 101347. [[CrossRef](#)]
28. Bu, J.; Bai, P.; Sharratt, P. Carbon Dioxide Capture with Regeneration of Salt. 2012.
29. Arce, G.L.A.F.; Soares Neto, T.G.; Ávila, I.; Luna, C.M.R.; Carvalho, J.A. Leaching optimization of mining wastes with lizardite and brucite contents for use in indirect mineral carbonation through the pH swing method. *J. Clean. Prod.* **2017**, *141*, 1324–1336. [[CrossRef](#)]
30. Stokreef, S.; Sadri, F.; Stokreef, A.; Ghahreman, A. Mineral Carbonation of Ultramafic Tailings: A Review of Reaction Mechanisms and Kinetics, Industry Case Studies, and Modelling. *Clean. Eng. Technol.* **2022**, *8*, 100491. [[CrossRef](#)]
31. Sanna, A.; Gaubert, J.; Maroto-valer, M.M. Alternative Regeneration of Chemicals Employed in Mineral Carbonation towards Technology Cost Reduction. *Chem. Eng. J.* **2016**, *306*, 1049–1057. [[CrossRef](#)]
32. Hitch, M.; Dipple, G.M. Economic Feasibility and Sensitivity Analysis of Integrating Industrial-Scale Mineral Carbonation into Mining Operations. *Miner. Eng.* **2012**, *39*, 268–275. [[CrossRef](#)]
33. Zhang, N.; Chai, Y.E.; Santos, R.M.; Šiller, L. Advances in Process Development of Aqueous CO₂ Mineralisation towards Scalability. *J. Environ. Chem. Eng.* **2020**, *8*, 104453. [[CrossRef](#)]
34. Bi, R.; Chen, C.; Tang, J.; Jia, X.; Xiang, S. Two-Level Optimization Model for Water Consumption Based on Water Prices in Eco-Industrial Parks. *Resour. Conserv. Recycl.* **2019**, *146*, 308–315. [[CrossRef](#)]
35. Sanna, A.; Steel, L.; Maroto-Valer, M.M. Carbon Dioxide Sequestration Using NaHSO₄ and NaOH: A Dissolution and Carbonation Optimisation Study. *J. Environ. Manag.* **2017**, *189*, 84–97. [[CrossRef](#)]
36. Daval, D.; Hellmann, R.; Martinez, I.; Gangloff, S.; Guyot, F. Lizardite Serpentine Dissolution Kinetics as a Function of PH and Temperature, Including Effects of Elevated P_{CO₂}. *Chem. Geol.* **2013**, *351*, 245–256. [[CrossRef](#)]
37. Teir, S.; Eloneva, S.; Fogelholm, C.-J.; Zevenhoven, R. Carbonation of Minerals and Industrial By-Products for CO₂ Sequestration. In Proceedings of the 3rd International Green Energy Conference, Västerås, Sweden, 18–20 June 2007.
38. Brown, T.L.; LeMay, E.; Bursten, B. *Química: A Ciência Central*, 9th ed.; Pearson Prentice Hall: São Paulo, Brazil, 2005; ISBN 85-87918-42-7.
39. Kola, A.K.; Mekala, M.; Goli, V.R. Experimental Design Data for the Biosynthesis of Citric Acid Using Central Composite Design Method. *Data Br.* **2017**, *12*, 234–241. [[CrossRef](#)]
40. Venkatesan, L.; Harris, A.; Greyling, M. Optimisation of Air Rate and Froth Depth in Flotation Using a CCRD Factorial Design—PGM Case Study. *Miner. Eng.* **2014**, *66–68*, 221–229. [[CrossRef](#)]
41. Mortari, D.A.; Ávila, I.; Crnkovic, P.M. Response Surface Methodology Applied to the Evaluation of the SO₂ Sorption Process in Two Brazilian Limestones. *Energy Fuels* **2013**, *27*, 2890–2898. [[CrossRef](#)]
42. Bösiger, P.; Richard, I.M.T.; Le Gat, L.; Michen, B.; Schubert, M.; Rossi, R.M.; Fortunato, G. Application of Response Surface Methodology to Tailor the Surface Chemistry of Electrospun Chitosan-Poly(Ethylene Oxide) Fibers. *Carbohydr. Polym.* **2018**, *186*, 122–131. [[CrossRef](#)]
43. Sanna, A.; Wang, X.; Lacinska, A.; Styles, M.; Paulson, T.; Maroto-Valer, M.M. Enhancing Mg Extraction from Lizardite-Rich Serpentine for CO₂ Mineral Sequestration. *Miner. Eng.* **2013**, *49*, 135–144. [[CrossRef](#)]
44. Arce, G.L.A.F.; Neto, T.G.S.; Ávila, I.; Luna, C.M.R.; dos Santos, J.C.; Carvalho, J.A. Influence of Physicochemical Properties of Brazilian Serpentinites on the Leaching Process for Indirect CO₂ Mineral Carbonation. *Hydrometallurgy* **2017**, *169*, 142–151. [[CrossRef](#)]
45. Hemmati, A.; Shayegan, J.; Sharratt, P.; Yeo, T.Y.; Bu, J. Solid Products Characterization in a Multi-Step Mineralization Process. *Chem. Eng. J.* **2014**, *252*, 210–219. [[CrossRef](#)]
46. Tutolo, B.M.; Luhmann, A.J.; Tosca, N.J.; Seyfried, W.E. Serpentinization as a Reactive Transport Process: The Brucite Silicification Reaction. *Earth Planet. Sci. Lett.* **2018**, *484*, 385–395. [[CrossRef](#)]
47. Hollingbery, L.A.; Hull, T.R. The Thermal Decomposition of Natural Mixtures of Huntite and Hydromagnesite. *Thermochim. Acta* **2012**, *528*, 45–52. [[CrossRef](#)]
48. Winnefeld, F.; Epifania, E.; Montagnaro, F.; Gartner, E.M. Further Studies of the Hydration of MgO-Hydromagnesite Blends. *Cem. Concr. Res.* **2019**, *126*, 105912. [[CrossRef](#)]
49. Azdarpour, A.; Asadullah, M.; Mohammadian, E.; Junin, R.; Hamidi, H.; Manan, M.; Rafizan, A.; Daud, M. Mineral Carbonation of Red Gypsum via PH-Swing Process: Effect of CO₂ Pressure on the Efficiency and Products Characteristics. *Chem. Eng. J.* **2015**, *264*, 425–436. [[CrossRef](#)]
50. Herring, A.; King, P.L.; Saadatfar, M.; Mahdini, F.; Kemis Yahyah, A.M.; Andò, E. 3D Microstructure Controls on Mineral Carbonation. *J. CO₂ Util.* **2021**, *47*, 101494. [[CrossRef](#)]
51. Maroto-Valer, M.M.; Fauth, D.J.; Kuchta, M.E.; Zhang, Y.; Andrésen, J.M. Activation of Magnesium Rich Minerals as Carbonation Feedstock Materials for CO₂ Sequestration. *Fuel Process. Technol.* **2005**, *86*, 1627–1645. [[CrossRef](#)]
52. Krevor, S.C.; Lackner, K.S. Enhancing Process Kinetics for Mineral Carbon Sequestration. *Energy Procedia* **2009**, *1*, 4867–4871. [[CrossRef](#)]

53. Pasquier, L.C.; Mercier, G.; Blais, J.F.; Cecchi, E.; Kentish, S. Technical & Economic Evaluation of a Mineral Carbonation Process Using Southern Québec Mining Wastes for CO₂ Sequestration of Raw Flue Gas with by-Product Recovery. *Int. J. Greenh. Gas Control* **2016**, *50*, 147–157. [[CrossRef](#)]
54. Zhang, J.; Zhang, R.; Geerlings, H.; Bi, J. Mg-Silicate Carbonation Based on an HCl- and NH₃-Recyclable Process: Effect of Carbonation Temperature. *Chem. Eng. Technol.* **2012**, *35*, 525–531. [[CrossRef](#)]

Disclaimer/Publisher’s Note: The statements, opinions and data contained in all publications are solely those of the individual author(s) and contributor(s) and not of MDPI and/or the editor(s). MDPI and/or the editor(s) disclaim responsibility for any injury to people or property resulting from any ideas, methods, instructions or products referred to in the content.